q-deformed spin foams for Riemannian quantum gravity

Igor Khavkine

Department of Applied Mathematics
University of Western Ontario
Canada

26 June 2007
LOOPS '07
UNAM Morelia, Mexico

based on *arXiv:0704.0278 [gr-qc]* (with Dan Christensen)

Outline

What?

- Barrett-Crane Model
- q-deformation

Why?

- Regularization
- Cosmological Constant

How?

- q-Barrett-Crane model
- Computer Simulation

So What?

- Results

Summary

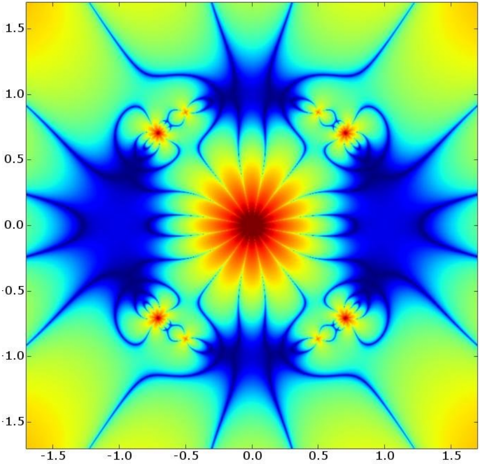

Spin Foams

Start with a triangulated 4-manifold T ($T^* \supset \Delta_n$ — the set of dual n-simplices). A *spin foam* is a coloring of the triangulation faces (Δ_2). A *spin foam model* assigns an amplitude to each spin foam F:

$$\mathcal{A}(F) = \prod_{f \in \Delta_2} A_F(f) \prod_{e \in \Delta_2} A_E(e) \prod_{v \in \Delta_1} A_V(v).$$

Also, to the triangulation as a whole and expectation values to observables

$$Z = \sum_F \mathcal{A}(F), \qquad \langle O \rangle = \frac{1}{Z} \sum_F O(F)\mathcal{A}(F).$$

Sum over all histories — discrete path integral!

Spin Foams

Start with a triangulated 4-manifold T ($T^* \supset \Delta_n$ — the set of dual n-simplices). A *spin foam* is a coloring of the triangulation faces (Δ_2). A *spin foam model* assigns an amplitude to each spin foam F:

$$\mathcal{A}(F) = \prod_{f \in \Delta_2} A_F(f) \prod_{e \in \Delta_2} A_E(e) \prod_{v \in \Delta_1} A_V(v).$$

Also, to the triangulation as a whole and expectation values to observables

$$Z = \sum_F \mathcal{A}(F), \qquad \langle O \rangle = \frac{1}{Z} \sum_F O(F)\mathcal{A}(F).$$

Sum over all histories — discrete path integral!

Goal — compute these sums numerically.

Barrett-Crane Model

A spin foam model for Riemannian General Relativity.

- Historically, obtained as a constrained version of discretized *BF* theory.
- Can also be derived from Group Field Theory.
- Specifies vertex amplitude (10*j symbol*):

$A_V(v) =$

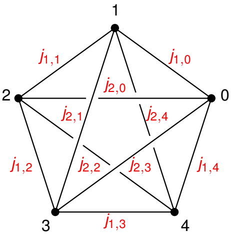

BC vertex — unique rotationally invariant.

The $j_{i,k}$ are balanced irreps $(j \otimes j)$ of $\mathrm{Spin}(4) \cong SU(2) \times SU(2)$.

- Several choices for amplitudes $A_F(f)$ and $A_E(e)$.

q-deformation

For $q = 1$, no deformation.

First, deal with $SU(2)$.

q-deformation

For $q = 1$, no deformation.

First, deal with $SU(2)$.

$U(\mathfrak{su}(2))$ generated by:

$$[\sigma_+, \sigma_-] = 4\sigma_3$$

$$[\sigma_3, \sigma_\pm] = \pm 2\sigma_\pm$$

q-deformation

For $q = 1$, no deformation.

First, deal with $SU(2)$.

$U(\mathfrak{su}(2))$ generated by:

$$[\sigma_+, \sigma_-] = 4\sigma_3$$

$$[\sigma_3, \sigma_\pm] = \pm 2\sigma_\pm$$

$U_q(\mathfrak{su}(2))$ generated by ($\Sigma \sim q^{\frac{1}{2}\sigma_3}$):

$$[\sigma_+, \sigma_-] = 4\frac{\Sigma^2 - \Sigma^{-2}}{q - q^{-1}}$$

$$\Sigma\sigma_\pm = q\sigma_\pm\Sigma$$

q-deformation

For $q = 1$, no deformation.

First, deal with $SU(2)$.

$U(\mathfrak{su}(2))$ generated by:

$$[\sigma_+, \sigma_-] = 4\sigma_3$$

$$[\sigma_3, \sigma_\pm] = \pm 2\sigma_\pm$$

Irreps classified by:

$$j = 0, \tfrac{1}{2}, 1, \tfrac{3}{2}, \ldots$$

$$\dim j = 2j + 1$$

$U_q(\mathfrak{su}(2))$ generated by ($\Sigma \sim q^{\frac{1}{2}\sigma_3}$):

$$[\sigma_+, \sigma_-] = 4\frac{\Sigma^2 - \Sigma^{-2}}{q - q^{-1}}$$

$$\Sigma\sigma_\pm = q\sigma_\pm\Sigma$$

q-deformation

For $q = 1$, no deformation.

First, deal with $SU(2)$.

$U(\mathfrak{su}(2))$ generated by:

$$[\sigma_+, \sigma_-] = 4\sigma_3$$

$$[\sigma_3, \sigma_\pm] = \pm 2\sigma_\pm$$

Irreps classified by:

$$j = 0, \tfrac{1}{2}, 1, \tfrac{3}{2}, \ldots$$

$$\dim j = 2j + 1$$

$U_q(\mathfrak{su}(2))$ generated by ($\Sigma \sim q^{\frac{1}{2}\sigma_3}$):

$$[\sigma_+, \sigma_-] = 4\frac{\Sigma^2 - \Sigma^{-2}}{q - q^{-1}}$$

$$\Sigma\sigma_\pm = q\sigma_\pm\Sigma$$

Irreps classified by (generic q):

$$j = 0, \tfrac{1}{2}, 1, \tfrac{3}{2}, \ldots$$

$$\dim j = 2j + 1$$

q-deformation

For $q = 1$, no deformation.

First, deal with $SU(2)$.

$U(\mathfrak{su}(2))$ generated by:

$$[\sigma_+, \sigma_-] = 4\sigma_3$$

$$[\sigma_3, \sigma_\pm] = \pm 2\sigma_\pm$$

Irreps classified by:

$$j = 0, \tfrac{1}{2}, 1, \tfrac{3}{2}, \ldots$$

$$\dim j = 2j + 1$$

$U_q(\mathfrak{su}(2))$ generated by ($\Sigma \sim q^{\frac{1}{2}\sigma_3}$):

$$[\sigma_+, \sigma_-] = 4\frac{\Sigma^2 - \Sigma^{-2}}{q - q^{-1}}$$

$$\Sigma\sigma_\pm = q\sigma_\pm\Sigma$$

Irreps classified by (generic q):

$$j = 0, \tfrac{1}{2}, 1, \tfrac{3}{2}, \ldots$$

$$\dim j = 2j + 1$$

ROU $q = e^{i\pi/r}$: $\quad j \leq \frac{r}{2} - 1$

q-deformation

For $q = 1$, no deformation.

First, deal with $SU(2)$.

$U(\mathfrak{su}(2))$ generated by:

$$[\sigma_+, \sigma_-] = 4\sigma_3$$

$$[\sigma_3, \sigma_\pm] = \pm 2\sigma_\pm$$

Irreps classified by:

$$j = 0, \tfrac{1}{2}, 1, \tfrac{3}{2}, \dots$$

$$\dim j = 2j + 1$$

$U_q(\mathfrak{su}(2))$ generated by ($\Sigma \sim q^{\frac{1}{2}\sigma_3}$):

$$[\sigma_+, \sigma_-] = 4\frac{\Sigma^2 - \Sigma^{-2}}{q - q^{-1}}$$

$$\Sigma\sigma_\pm = q\sigma_\pm\Sigma$$

Irreps classified by (generic q):

$$j = 0, \tfrac{1}{2}, 1, \tfrac{3}{2}, \dots$$

$$\dim j = 2j + 1$$

ROU $q = e^{i\pi/r}$: $\quad j \leq \frac{r}{2} - 1$

$$U(\mathfrak{spin}(4)) \cong U(\mathfrak{su}(2)) \oplus U(\mathfrak{su}(2))$$

q-deformation

For $q = 1$, no deformation.

First, deal with $SU(2)$.

$U(\mathfrak{su}(2))$ generated by:

$$[\sigma_+, \sigma_-] = 4\sigma_3$$

$$[\sigma_3, \sigma_\pm] = \pm 2\sigma_\pm$$

Irreps classified by:

$$j = 0, \tfrac{1}{2}, 1, \tfrac{3}{2}, \ldots$$

$$\dim j = 2j + 1$$

$U_q(\mathfrak{su}(2))$ generated by ($\Sigma \sim q^{\frac{1}{2}\sigma_3}$):

$$[\sigma_+, \sigma_-] = 4\frac{\Sigma^2 - \Sigma^{-2}}{q - q^{-1}}$$

$$\Sigma\sigma_\pm = q\sigma_\pm\Sigma$$

Irreps classified by (generic q):

$$j = 0, \tfrac{1}{2}, 1, \tfrac{3}{2}, \ldots$$

$$\dim j = 2j + 1$$

ROU $q = e^{i\pi/r}$: $\quad j \leq \frac{r}{2} - 1$

$$U(\mathfrak{spin}(4)) \cong U(\mathfrak{su}(2)) \oplus U(\mathfrak{su}(2))$$

$$U_{q,q'}(\mathfrak{spin}(4)) \cong U_q(\mathfrak{su}(2)) \oplus U_{q'}(\mathfrak{su}(2))$$

q-deformation

For $q = 1$, no deformation.

First, deal with $SU(2)$.

$U(\mathfrak{su}(2))$ generated by:

$$[\sigma_+, \sigma_-] = 4\sigma_3$$

$$[\sigma_3, \sigma_\pm] = \pm 2\sigma_\pm$$

Irreps classified by:

$$j = 0, \tfrac{1}{2}, 1, \tfrac{3}{2}, \ldots$$

$$\dim j = 2j + 1$$

$U_q(\mathfrak{su}(2))$ generated by ($\Sigma \sim q^{\frac{1}{2}\sigma_3}$):

$$[\sigma_+, \sigma_-] = 4\frac{\Sigma^2 - \Sigma^{-2}}{q - q^{-1}}$$

$$\Sigma\sigma_\pm = q\sigma_\pm\Sigma$$

Irreps classified by (generic q):

$$j = 0, \tfrac{1}{2}, 1, \tfrac{3}{2}, \ldots$$

$$\dim j = 2j + 1$$

ROU $q = e^{i\pi/r}$: $\quad j \leq \frac{r}{2} - 1$

$$U(\mathfrak{spin}(4)) \cong U(\mathfrak{su}(2)) \oplus U(\mathfrak{su}(2)) \qquad U_{q,q'}(\mathfrak{spin}(4)) \cong U_q(\mathfrak{su}(2)) \oplus U_{q'}(\mathfrak{su}(2))$$

Spin networks: graphs $\longrightarrow$ ribbon graphs.

Regularization

Application of q-deformation.

- For q a root of unity (ROU) the number of irreps is finite. Partition function Z is automatically finite.

Regularization

Application of q-deformation.

- For q a root of unity (ROU) the number of irreps is finite. Partition function Z is automatically finite.
- Ponzano-Regge model for 3-d Riemannian GR (1968). An early spin foam model — divergent.
- At a *ROU* q, this model is regularized. Constructed by Turaev and Viro as a state sum for 3-manifold invariants (1992).

Regularization

Application of q-deformation.

- For q a root of unity (ROU) the number of irreps is finite. Partition function Z is automatically finite.
- Ponzano-Regge model for 3-d Riemannian GR (1968). An early spin foam model — divergent.
- At a *ROU* q, this model is regularized. Constructed by Turaev and Viro as a state sum for 3-manifold invariants (1992).

- DFKR model (Barrett-Crane variation due to De Pietri, Freidel, Krasnov & Rovelli, 1999) — also divergent, discovered from numerical investigation (2002).
- At a *ROU* q, the DFKR model is also regularized.

Cosmological Constant

Application of q-deformation.

In Loop Quantum Gravity, $SU(2)$ spin networks are embedded in a spatial slice.

- The spin network basis describes states of quantum spatial geometry.

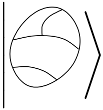

Cosmological Constant

Application of q-deformation.

In Loop Quantum Gravity, $SU(2)$ spin networks are embedded in a spatial slice.

- The spin network basis describes states of quantum spatial geometry.

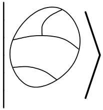

- Kodama state $|\mathcal{K}; \Lambda\rangle$ — approximates deSitter space, a vacuum with positive Cosmological Constant, $\Lambda > 0$.
- Smolin (1995) argues that invariance under large gauge transformations discretizes the CC, $\Lambda \sim 1/r$.

Cosmological Constant

Application of q-deformation.

In Loop Quantum Gravity, $SU(2)$ spin networks are embedded in a spatial slice.

- The spin network basis describes states of quantum spatial geometry.

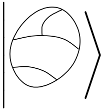

- Kodama state $|\mathcal{K}; \Lambda\rangle$ — approximates deSitter space, a vacuum with positive Cosmological Constant, $\Lambda > 0$.
- Smolin (1995) argues that invariance under large gauge transformations discretizes the CC, $\Lambda \sim 1/r$.
- Expansion coefficients give topological link and graph invariants:

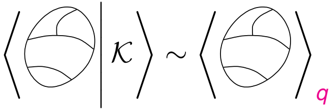

- With precisely $q = \exp(i\pi/r)$!

q-Barrett-Crane model

- Ingredients for q-deformation have been in the literature for some time.

q-Barrett-Crane model

- Ingredients for q-deformation have been in the literature for some time.
- A special family of deformations (Yetter, 1999):

$$U_{q,q^{-1}}(\mathfrak{spin}(4)) \cong U_q(\mathfrak{su}(2)) \oplus U_{q^{-1}}(\mathfrak{su}(2)).$$

BC vertex still rotationally invariant, ribbon structure trivial.

q-Barrett-Crane model

- Ingredients for q-deformation have been in the literature for some time.
- A special family of deformations (Yetter, 1999):

$$U_{q,q^{-1}}(\mathfrak{spin}(4)) \cong U_q(\mathfrak{su}(2)) \oplus U_{q^{-1}}(\mathfrak{su}(2)).$$

  BC vertex still rotationally invariant, ribbon structure trivial.
- Intersection structure of $10j$ symbol (only non-planar spin network) fixed from the Crane-Yetter model (1994)

q-Barrett-Crane model

- Ingredients for q-deformation have been in the literature for some time.
- A special family of deformations (Yetter, 1999):

$$U_{q,q^{-1}}(\mathfrak{spin}(4)) \cong U_q(\mathfrak{su}(2)) \oplus U_{q^{-1}}(\mathfrak{su}(2)).$$

  BC vertex still rotationally invariant, ribbon structure trivial.
- Intersection structure of $10j$ symbol (only non-planar spin network) fixed from the Crane-Yetter model (1994):

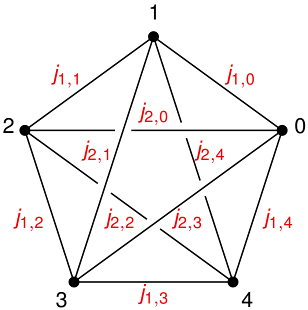

- Retains permutation symmetry.
- Christensen-Egan (2002) efficient algorithm generalizes.

Computer Simulation

- Implement $U_q(\mathfrak{su}(2))$ spin network evaluations — $|q| > 1$ numerically unstable! But ROU q is OK.

Computer Simulation

- Implement $U_q(\mathfrak{su}(2))$ spin network evaluations — $|q| > 1$ numerically unstable! But ROU q is OK.

tetrahedral network vs. q

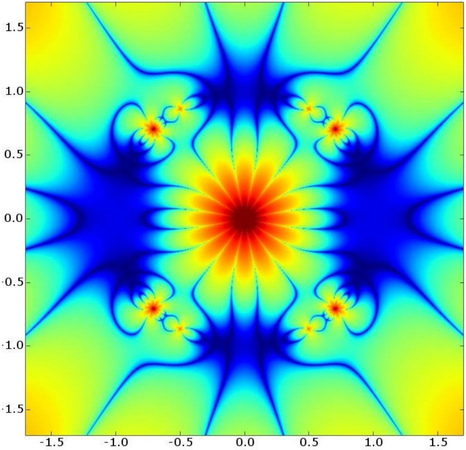

Computer Simulation

- Implement $U_q(\mathfrak{su}(2))$ spin network evaluations — $|q| > 1$ numerically unstable! But ROU q is OK.

- Evaluate partition function and observables using importance sampling (Metropolis algorithm):

$$\langle O \rangle = \frac{1}{Z} \sum_{F} O(F)\mathcal{A}(F).$$

Computer Simulation

- Implement $U_q(\mathfrak{su}(2))$ spin network evaluations — $|q| > 1$ numerically unstable! But ROU q is OK.

- Evaluate partition function and observables using importance sampling (Metropolis algorithm):

$$\langle O \rangle = \frac{1}{Z} \sum_{F} O(F)\mathcal{A}(F).$$

- Elementary move — add closed bubble in dual skeleton.

Computer Simulation

- Implement $U_q(\mathfrak{su}(2))$ spin network evaluations — $|q| > 1$ numerically unstable! But ROU q is OK.

- Evaluate partition function and observables using importance sampling (Metropolis algorithm):

$$\langle O \rangle = \frac{1}{Z} \sum_F O(F) \mathcal{A}(F).$$

- Elementary move — add closed bubble in dual skeleton.

- Works well since $\mathcal{A}(F) \geq 0$ when $q = 1$ or ROU, in the absence of boundaries.

Models

Perez-Rovelli (2000):

$A_F(f) =$ 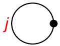

, $A_E(e) =$ 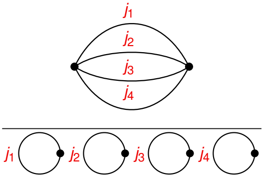

.

DFKR (2000):

$A_F(f) =$ 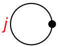

, $A_E(e) =$ 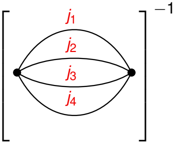

.

Baez-Christensen (2002):

$A_F(f) = 1,$ $A_E(e) =$ 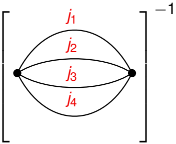

.

Observables

Spin foam observables depend on face spin labels:

spin avg. $$J(F) = \frac{1}{|\Delta_2|} \sum_{f \in \Delta_2} \lfloor j(f) \rceil \,,$$

spin var. $$(\delta J)^2(F) = \frac{1}{|\Delta_2|} \sum_{f \in \Delta_2} \left(\lfloor j(f) \rceil - \langle J \rangle \right)^2 \,,$$

area avg. $$A(F) = \frac{1}{|\Delta_2|} \sum_{f \in \Delta_2} \sqrt{\lfloor j(f) \rceil \, \lfloor j(f) + 1 \rceil},$$

spin corr. $$C_d(F) = \frac{1}{N_d} \sum_{\mathrm{dist}(f,f')=d} \frac{\lfloor j(f) \rceil \, \lfloor j(f') \rceil - \langle J \rangle^2}{\left\langle (\delta J)^2 \right\rangle}.$$

Quantum half integers $\lfloor j \rceil = j$ when $q = 1$, but $\lfloor j \rceil \sim \sin(2j\pi/r)$ when $q = e^{i\pi/r}$.

Observables Discontinuous as $r \to \infty$

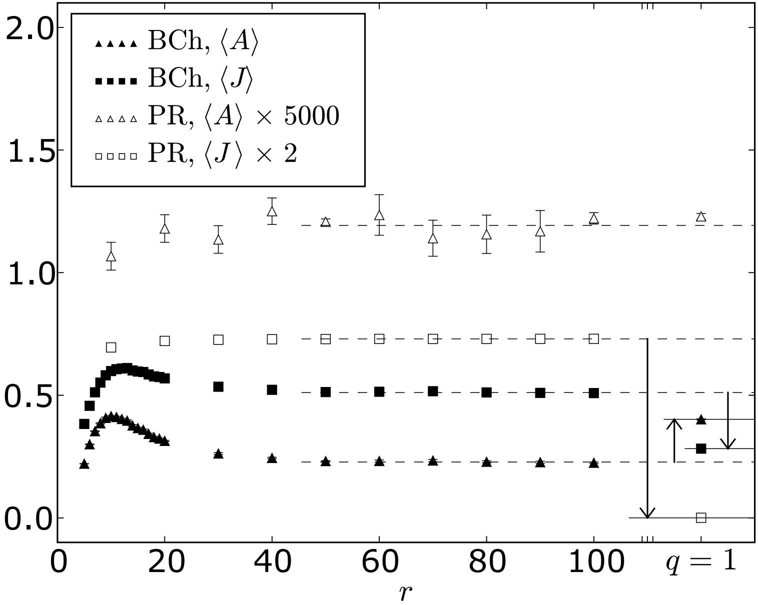

Single Spin Distribution

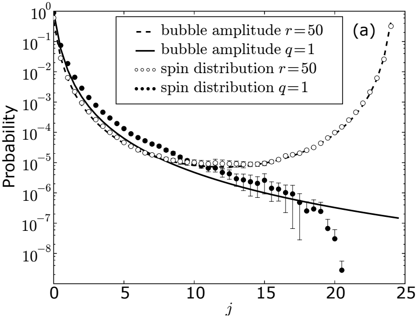

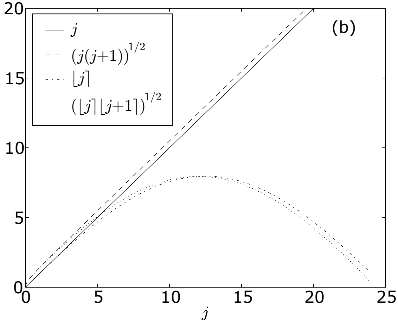

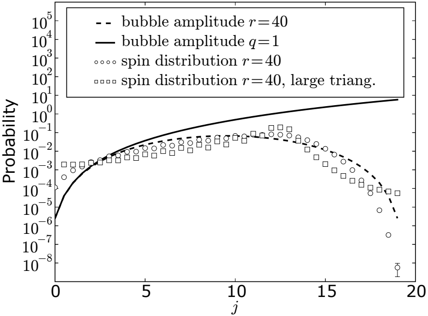

- SSD — frequency of occurence of j.
- BA — $\mathcal{A}(F)$, where F contains minimal bubble.

Single Spin Distribution

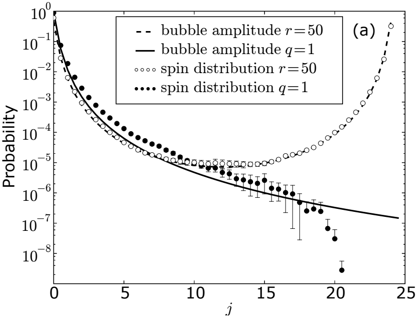

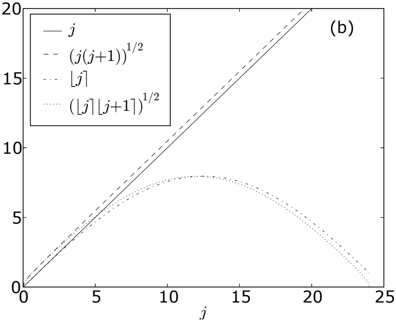

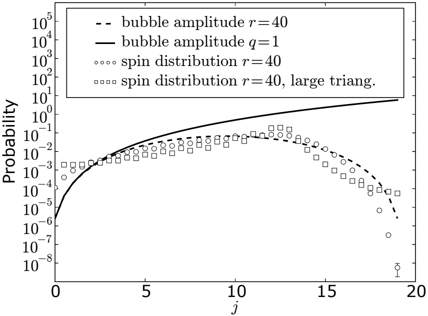

- SSD — frequency of occurence of j.
- BA — $\mathcal{A}(F)$, where F contains minimal bubble.
- For PR and BCh, bubbles dominate!

Single Spin Distribution

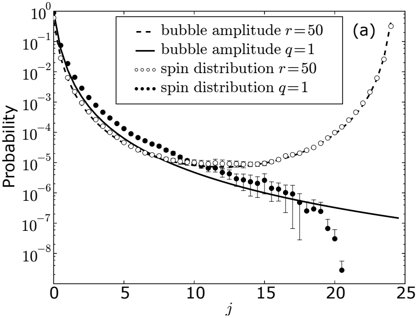

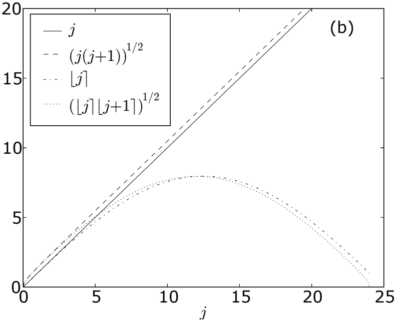

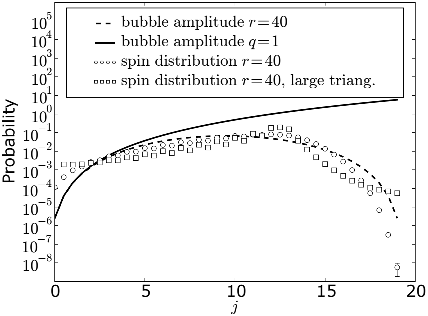

- SSD — frequency of occurence of j.
- BA — $\mathcal{A}(F)$, where F contains minimal bubble.
- For PR and BCh, bubbles dominate!
- Not for DFKR.

Spin Correlation

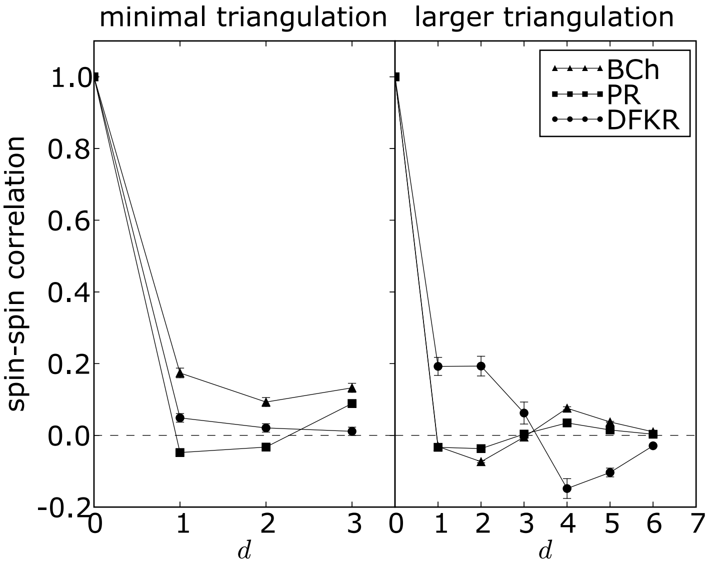

Consistent with isolated bubble hypothesis.

Summary and Outlook

- Computer simulation of q-Barrett-Crane models now possible and practical, for modest sized triangulations.

Summary and Outlook

- Computer simulation of q-Barrett-Crane models now possible and practical, for modest sized triangulations.
- Observables show a discontinuity as $q \to 1$ through roots of unity. At odds with cosmological constant interpretation.

Summary and Outlook

- Computer simulation of q-Barrett-Crane models now possible and practical, for modest sized triangulations.
- Observables show a discontinuity as $q \to 1$ through roots of unity. At odds with cosmological constant interpretation.
- BC models show strong dependence on edge and face amplitudes.

Summary and Outlook

- Computer simulation of q-Barrett-Crane models now possible and practical, for modest sized triangulations.
- Observables show a discontinuity as $q \to 1$ through roots of unity. At odds with cosmological constant interpretation.
- BC models show strong dependence on edge and face amplitudes.

- Outlook
  - Simulations with $|q| \sim 1$.
  - Spin correlation on larger triangulations.
  - Lorentzian signature.

Summary and Outlook

- Computer simulation of q-Barrett-Crane models now possible and practical, for modest sized triangulations.
- Observables show a discontinuity as $q \to 1$ through roots of unity. At odds with cosmological constant interpretation.
- BC models show strong dependence on edge and face amplitudes.

- Outlook
  - Simulations with $|q| \sim 1$.
  - Spin correlation on larger triangulations.
  - Lorentzian signature.

Thank you for your attention!